INSTITUTE OF PHYSICS PUBLISHING CLASSICAL AND QUANTUM GRAVITY

Class. Quantum Grav. **18** (2001) 2487–2498 www.iop.org/Journals/cq PII: S0264-9381(01)24077-5

The MICROSCOPE space mission

Pierre Touboul and Manuel Rodrigues

Physics et Instrumentation Departement, Office National d'Etudes et de Recherches Aérospatiales, BP 72, 92322 Châtillon Cedex, France

Received 10 April 2001

Abstract

The MICROSCOPE mission aims to test the equivalence principle (EP) up to an accuracy of 10^{-15} using its well known manifestation: the universality of free-fall. The mission, implemented in the Cnes programme of 2000, schedules the launch of the microsatellite for 2004. The satellite payload comprises four gravitational sensors operating at finely stabilized room temperature. The masses of the sensors are controlled to the same orbital motion on-board the satellite, which compensates external surface forces in real time by actuation of electrical thrusters. Accurate measurements of the electrostatic forces applied to the masses, so that they follow the same gravitational orbit, are processed in order to reject any common effects on the masses; then the differential outputs are observed with high precision along the Earth-pointing axis, with an expected resolution of 5×10^{-15} m s^{-2}. The quasi cylindrical test masses are concentric in order to reject gravity gradient effects, and are made of platinum or titanium alloys. The instrument's concept and design are presented, and the rationale of the space experiment is explained.

PACS number: 0480C

(Some figures in this article are in colour only in the electronic version; see `www.iop.org`)

1. MICROSCOPE mission rationale

Over the previous two decades much effort has been expended in physics laboratories on the development of experiments dealing with the test of the equivalence principle (EP), or on the search for new interactions or a new gravitational potential.

Improvement in the confirmation of the equivalence between inertial mass and gravitational mass represents an important verification of the relativistic theory of gravitation, and of other metric theories which postulate this principle, and it should excite interest in more accurate experiments for the determination of post-Newtonian coefficients [1, 2]. A violation of the equivalence principle, which is an exact identity for general relativity, would certainly lead to evidence for a new interaction—as predicted by many current quantum theories of gravity [3–5]. An extra massless scalar field that naturally violates the EP needs to be illuminated through experimentation such as the EP test, which is one of the most sensitive low-energy probes.

The most accurate laboratory experiments to date exploit torsion pendulums, and have to deal with environmental instabilities induced, in particular, by the Earth's gravity gradient fluctuations [6], and by human activities. Important results have also been obtained by considering the Earth–Moon relative motion in the Sun's gravity field, accurately measured by laser ranging, but the material composition of the two celestial bodies is not sufficiently well identified [7] to interpret the results.

Many space experiments have also been studied and proposed over the past years, but these missions have not yet been selected because they have been considered by the space agencies to be too complex, difficult to implement and expensive [8–11].

The MICROSCOPE space mission (MICROSatellite pour l'Observation du Principe d'Equivalence) is the first selected mission aimed at an EP test, with a satellite to be launched in 2004, and an expected accuracy of at least 10^{-15}. This mission takes advantage of specific competences developed in Onera, in the 'Côte d'Azur' Observatory, and in Cnes. Three-axis electrostatic accelerometers, recently produced for space applications, can exhibit at room temperature ultra-high sensitivities compatible with femto-g resolution [12]. Recent altimetry and geodesy missions [13, 14] have led to global and accurate Earth gravity field determination, expressed in terms of spherical harmonic series, and to the production of dedicated mathematical and computational tools for the simulation of accurate orbital motion. Micro-satellites are now available with low-cost launch opportunities, such as being a secondary passenger on Ariane V, for instance, the satellite mass here being restricted to less than 120 kg—allowing for a payload of about 40 kg, 50 l and 40–50 W.

In the MICROSCOPE experiment the Earth is the gravitational source, and the free-fall motion of two masses, composed of two different materials, is observed and controlled, taking care that both masses are subjected to exactly the same gravitational field. The controlled electrostatic field, added to break the experimental symmetry by forcing the masses to remain on the same orbit, is accurately measured: any defect of symmetry gives rise to evidence of an EP violation.

This space experiment exploits the very 'soft' accelerometric environment delivered on-board a dedicated compact satellite that includes a drag compensation system: the surface

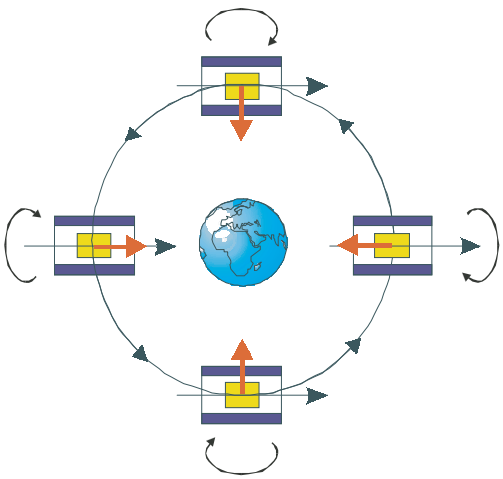

Figure 1. The MICROSCOPE experimental concept: the two masses fall around the Earth, controlled along the same orbit; in the case of an EP violation the electrostatic force (in grey) is accurately measured along the rotating instrument frame (in black).

forces applied to the satellite are counteracted continuously by the thrust of the electrical propulsion system.

The observation period in steady conditions of the motions of the masses in free-fall leads to an expected integration of signal over days and weeks, and thus to a high level of rejection of stochastic disturbances. Rotations of the observational frame with respect to the Earth's gravity field frame also help in the discrimination of an eventual EP violation signal from instrumental and environmental sources of noise. Several rotation frequencies are considered around 10^{-3} Hz, with well selected phases with respect to the satellite position on its orbit: frequency analyses with heterodyne detection are then considered for the data processing, 1% stability of the rotation rate being required.

2. Mission overview

The satellite payload is, in fact, composed of two quite identical instruments, each containing two concentric test masses. The masses are made of the same material in the 'first' instrument, which is dedicated to assessing the accuracy of the EP experiment. The masses' materials are different in the 'second' instrument. Then, in order to suppress systematic errors, the experimental logic relies on the double comparison of the outputs of two pairs of electrostatic accelerometers, the inertial masses of which are the test masses.

The selection of the masses' material is a compromise between the instrumental accuracy requirements and the theoretical interest. Micrometric geometry, thermal stability and ageing; magnetic and electric properties; and out-gassing, and chemical stability are properties to be considered, as well as differences of nuclear components related to new possible interactions [5], or to already performed EP tests [6]. Platinum is presently selected for three of the masses and titanium for the last one. The weight of the masses ranges from 0.4 kg up to 1.7 kg. More pairs of masses and materials are obviously of great interest, but they are not compatible with the integration of more instruments on-board the microsatellite. The success of the mission will certainly open the door to further missions.

The mass motions are to be measured with high precision by capacitive position sensing with respect to the same highly stable silica instrument frame, and with an accuracy of 3×10^{-11} m Hz$^{-1/2}$. This motion can be simply expressed as

$$m_{I_A}\left(\ddot{X}_A + \ddot{x}_A\right) - m_{g_A} g_A = F_A + F_{p_A}$$

with the index A (or B, later) for the mass under consideration, the index I or g for inertial or gravitational mass, X the displacement of the instrument structure (linked to the satellite) with respect to the inertial frame and x that of the mass with respect to the instrument. g_A is the Earth's gravitational field integrated over the mass volume, and F_A and F_{PA} are the applied forces due, respectively, to the electrostatic generated field, and to disturbing sources.

The relative position of the two masses is maintained fixed. The fine comparison of the electrostatic control forces, performed with an accuracy of 5×10^{-13} N Hz$^{-1/2}$, leads to an EP test with the expected 10^{-15} accuracy—considering an integrating period of about 1 d.

The following expression for the measurement, as provided by the instrument, shows the major terms to be optimized in the experiment:

$$\frac{\hat{F}_A}{m_{I_A}} = (I + K_A)F_A + E(F_A) + E_{n_A} \qquad \text{with} \quad \frac{\hat{F}_A}{m_{I_A}}$$

which is the measure of the electrostatic acceleration applied to the mass A; I and K are the identity and sensitivity matrices, respectively, $E(F_A)$ is the nonlinear term, and E_{nA} is the

noise of the pick-up measurement device. Then

$$\frac{\hat{F}_A}{m_{I_A}} - \frac{\hat{F}_B}{m_{I_B}} \approx +(K_A - K_B)\frac{\ddot{X}_A + \ddot{x}_A + \ddot{X}_B + \ddot{x}_B}{2} + \left(I + \frac{(K_A + K_B)}{2}\right)\left(\ddot{X}_A - \ddot{X}_B\right)$$
$$+\left(I + \frac{(K_A + K_B)}{2}\right)\left\{\left(\overset{\circ\circ}{x}_A - \overset{\circ\circ}{x}_B\right) + 2\Omega\left(\overset{\circ}{x}_A - \overset{\circ}{x}_B\right) + \left(\Omega \times \Omega + \dot{\Omega}\right)(x_A - x_B)\right\}$$
$$-\frac{1}{2}\left(\frac{m_{g_A}}{m_{I_A}} + \frac{m_{g_B}}{m_{I_B}}\right)(g_A - g_B) - \frac{\hat{F}_{pA}}{m_{I_A}} + \frac{\hat{F}_{pB}}{m_{I_B}}$$
$$+E(F_A) - E(F_B) + E_{n_A} - E_{n_B} - \left(\frac{m_{g_A}}{m_{I_A}} - \frac{m_{g_B}}{m_{I_B}}\right)\left(\frac{g_A + g_B}{2}\right).$$

The first term corresponds to the common-mode acceleration which is not fully suppressed. The second and third terms to the relative residual motion of the masses and to the effect of the attitude variations, where Ω is the angular velocity of the instrument about the drag-free point (the derivatives in the third term are performed in the rotating frame). The fourth term corresponds to the gravity gradient, and the last term to the EP test: the term to be accurately determined.

The attitude as well as the atmospheric and thermal drag of the satellite are actively controlled in such a way that the satellite follows the two test masses in their gravitational motion.

Field emission electric propulsion (FEEP) [15, 16] thrusters are to be used to generate continuously modulated thrust during the measurement mode, when the satellite shields the instrument from the Earth's and solar radiation pressures, and from atmospheric drag. The propulsion system also allows a fine calibration of the instrument by generating well known kinematic accelerations in all six degrees of freedom. This enables verification of the alignments of the sensitive axes, and the matching of the instrumental sensitivities necessary to reject common kinematic acceleration fields ($K_{A_{ij}} - K_{B_{ij}} < 10^{-4}$).

The satellite's orbital altitude must be sufficiently high so as to reduce the atmospheric drag that must be compensated by the electrical thrusters, but this reduces the strength of the gravity field. Hence, an altitude of around 700 km has been selected ($g \approx 8\ \mathrm{m\ s^{-2}}$), where the accelerations due to the drag and to the solar radiation pressure are expected to be of the same order.

The selection of a 6–18 h helio-synchronous orbit leads to avoidance of the fluctuations of the Sun's orientation and the eclipse, reducing the temperature variations and the thermoelastic structural constraints which can generate acceleration spikes.

The eccentricity of the quasi-circular orbit must be sufficiently small to concentrate the power spectrum of the Earth's monopolar gravity field into one major spectral line. Furthermore, the fluctuations of the gravity gradient in the instrument frame have to be limited to the same spectral line.

The perturbing effects of the satellite and the Earth's gravity gradient are of special importance. The cylindrical test masses present sphere-like inertia matrices to limit these effects, and the off-centring of the two masses is limited by construction to 20 μm; gravitational attractions are then equal on both masses with an accuracy of better than one part per 1000, which is sufficient for the experiment, given its environment. Moreover, this in-orbital-plane off-centring can be evaluated through the effect of the gravity gradient's major component with an accuracy of better than 10^{-7} m; the gravity gradient is observed at twice the frequency of the gravity field. Thus the eccentricity must be smaller than 5×10^{-3} to limit the disturbing difference of accelerations induced by the gravity gradients in the case of zero satellite spin.

In this process, knowledge of the satellite position is necessary in order to compute the gravity gradient: 300 m can be achieved along the three directions and this appears to be sufficient.

The out-of-plane off-centring cannot be estimated through in-orbit data analysis; thus the 20 μm initial value has to be considered when specifying the instrumental axis direction in the orbital plane. The instrument frame, orbital plane and rotation axis, all will be aligned to within a few 10^{-3} rad accuracy.

The mission duration is to be 1 yr. After the orbital injection the satellite is to be controlled in 'safe mode', Earth-pointing, using the nominal equipment of the micro-satellite platform: Sun sensor and star tracker, magneto-torquers and reaction wheels. Then, the two instruments are to be switched-on, one by one, their proper operation being verified, and the satellite electrical propulsion being calibrated by the accelerometer data. The satellite's mass centring and its structural behaviour are to be verified before switched on of the drag-free and fine attitude control. The accelerometers are then to be submitted to very weak accelerations and their mode of highest sensitivity is to be switched-on; the instruments and the satellite control are then to be accurately characterized in terms of: residual acceleration levels, stability of rotation axis and frequency, coupling between axes, and instrumental sensitivity to environmental and gravity gradients. After calibration, the EP experiment is to be realized with the first instrument in inertial and rotating attitudes, and with two angular phases along the orbit (defined at the equator passage). The drag-free system will null the common measured accelerations of this instrument, the second instrument being used to control the attitude and to monitor all applied levels. In order to verify that no severe drifts have occurred between the beginning and the end of the experiment, the previous phase of calibration will be performed again. The EP experiment will then be performed with the second instrument, with a new calibration at the end. According to the required integration periods for the filtering of the data, the minimum duration of the overall procedure is evaluated to be 6 months. The extra time will be used to assess the experiment and to perform complementary operations.

The scientific mission centre will be located at the Onera laboratory, and will be in charge of: pre-processing and storage of the scientific and housekeeping data, the sending of telecommands, the partial processing of the measurements for a first 'fast overview' of the experiment, and the management of exchanges between Onera and Observatoire de la Côte d'Azur for the fine analysis. The total data flow rate is evaluated to 5.5 kbit s^{-1}—less than 480 Mbit per day. The satellite's memory capacity of 1 Gb and the rate of the TM/TC link to the ground station of 400 kbit s^{-1} are compatible with the payload needs.

3. The MICROSCOPE instrument

The instrument, specifically designed for the mission, has been derived from the cryogenic instrument studied in the past for the GEOSTEP mission aiming at the EP test with a better accuracy of 10^{-17}, but requiring at least a 400 kg satellite [9].

Each instrument is composed of two concentric electrostatic accelerometers (see figure 2). The test masses of each accelerometer are integrated at the centre of the fused silica instrument cage. Electrodes are engraved all around each mass in the gold coatings deposited on the cage. The electrode set configuration presents an axial and a radial symmetry.

Pairs of electrodes are used for the capacitive sensing of the mass position and attitude along the three axes. The eight quadrant electrodes pertain to the radial translations and rotations, the two cylindrical sensing electrodes at the ends of the test mass being used for the axial direction. The rotation of the mass about the axial direction is measured through dedicated flat areas on the mass and attendant external electrodes.

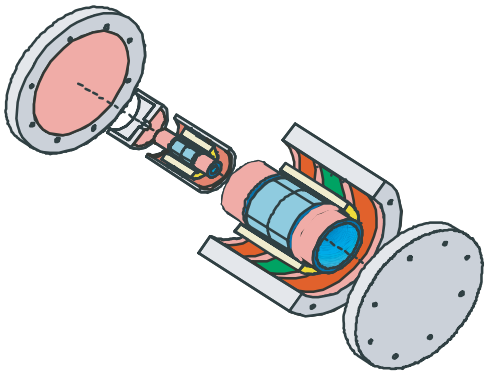

Figure 2. Differential accelerometer sketch; the two masses (light-grey) are integrated each inside a silica core composed of inner and the outer cylinders which carry the electrodes (radial in mid-grey and axial dark-grey).

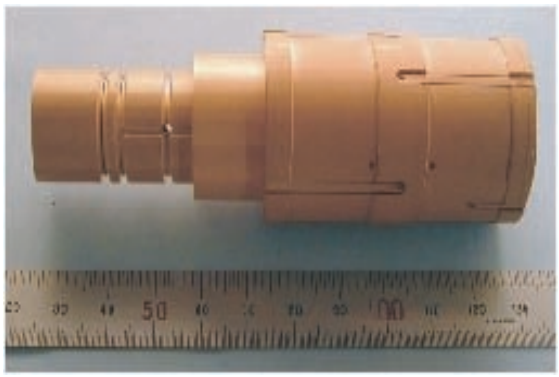

Figure 3. Prototype of one electrostatic accelerometer core: the inner gold-coated silica cylinder carries the radial electrodes; the silica mass is also gold coated and included inside the outer cylinder.

This electrode configuration is optimized from the point of view of reducing the electrostatic stiffness and damping associated with mass-motion along the axial direction. Such effects may be induced by the sensing electrical signals between the mass and the instrument frame for a range of mass positions along this axis. The back-action of the capacitive sensing has to be reduced in consideration of induced disturbing accelerations being applied to the mass along the axial direction.

From the position sensing, a dedicated set of voltages are computed and applied, when needed, and on the same electrodes, to generate an all-round electrostatic field. Each mass can then be controlled motionless with respect to the same silica instrument frame. The resultant of the generated electrostatic forces is derived from the accurate measurement of the applied voltages (see figure 4).

The mean force applied to both masses is, in fact, maintained at a null by the satellite drag compensation system, which acts on the thrusters so as to move the satellite and so the instrument silica frame follows the masses; the difference of the electrostatic forces is then observed along the orbit in the search of any EP-violating signal.

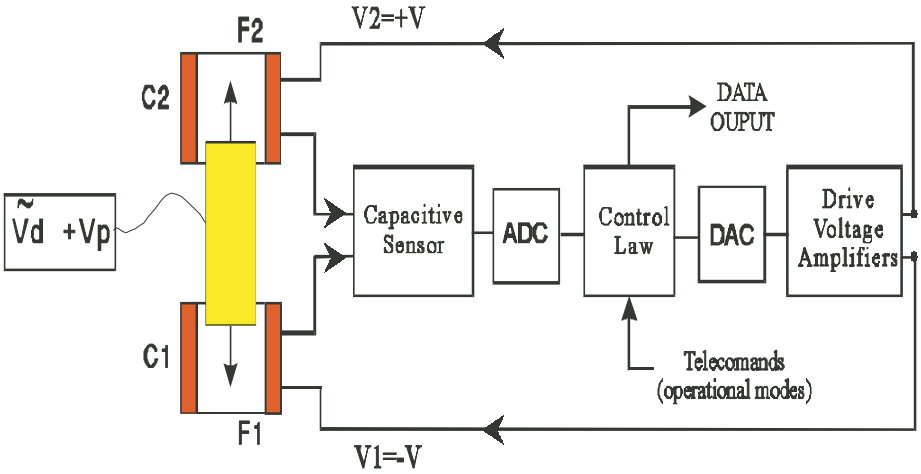

Figure 4. Electrostatic loop configuration: the capacitances C_1 and C_2 are maintained equal by applying the voltages V_1 and V_2 to move the mass to the centre.

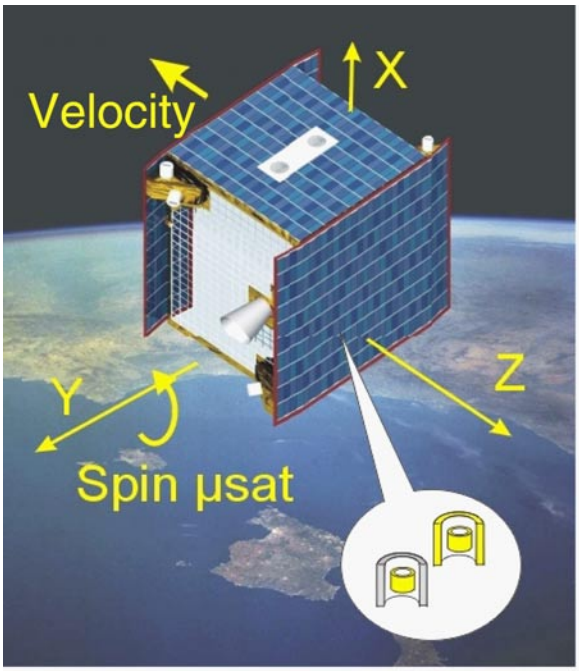

Figure 5. General configuration of the MICROSCOPE satellite in orbit (courtesy of Cnes).

The relative position of the masses can be modified by offsetting the electrostatic servo-loops: verification of the instrument sensitivity to this parameter will be performed during the calibration phase as well as its rejection rate of the Earth's gravity gradient signal.

Both instrument cores are integrated in vacuum-tight housings that also provide thermal insulation and magnetic shielding if necessary: fluctuations of the instrument temperature will be less than 0.1 K over one orbit, and the distribution of the temperature inside the housing

will be managed so as to be less than 1 K m^{-1}—thanks to the insulation and relatively high thermal inertia of each core.

These housings are to be mounted near the satellite's centre of mass, but no stringent requirement is considered necessary: the rotation of the satellite is to be controlled through the instrumental outputs, maintaining the DC value at a null and thereby the mass centres on the rotational axis. Thus, the satellite centre of mass is located near the test mass centres only in order to reduce the torque demanded by the propulsion systems for maintenance of the satellite's rotation.

The accelerometer sensitive axes are oriented in the orbital plane along the spacecraft X-axis (see figure 5), the centres of the test masses both being on the rotating axis of the satellite, normal to the orbital plane. The total mass of the payload is estimated to 40 kg, including the two instrument cores and the electronics unit—which consumes an overall power of less than 40 W (both instruments operating).

4. The MICROSCOPE satellite

The micro-satellite design is compatible with the selected Ariane V opportunity of launch, as a complementary passenger to the French HELIOS 2 main satellite, scheduled for mid 2004. The general configuration of the satellite is presented in figure 5. This satellite is the fourth of the specific Cnes production line, but the MICROSCOPE experiment requires a dedicated configuration.

The satellite is essentially cubic, 60 cm on a side, and is rigid and compact with no deployable solar panel. Any mass motion on-board is avoided and no momentum wheel is used during the experiment's operation. The thermoelastic behaviour of the satellite will be carefully optimized to avoid variations of stress and vibrations. The structure is to be realized with aluminium honeycomb and plates. The three solar panels are mounted on three faces of the bus with high-efficiency AsGa solar cells. The available power of 80 W will be shared by the payload, the satellite module and the electrical propulsion system.

The magnetic cleanliness of the satellite has been considered and the residual moment should be less than 1 A m^2. Furthermore, the magnetic moments on-board the satellite will be steady, and variations of less than 0.1 A m^2 at 30 cm from the instrument are specified to limit magnetic disturbances due to test-mass susceptibility. This concerns particularly the magneto-torquers and the batteries. Thermal stability of the apparatus is required, and, from the developed thermal model, the figures in table 1 will be taken into consideration.

During the mission, the satellite will be Earth-pointing, inertial-pointing or rotating about the Y-axis, normal to the orbital plane, with rather low angular rates of about 4×10^{-3} rad s^{-1}. The frequency f_{EP}, at which the experiment will be realized, is then the sum of the orbital

Table 1. Thermal environment specifications, power spectral density (PSD) and tone variations.

	Electronics unit	Mechanical unit
Operating temperature	+10 °C–+50 °C	+20 °C–+40 °C
Thermal variations		
PSD (about f_{EP})	1 K $Hz^{-1/2}$	1 K $Hz^{-1/2}$
Tone (sine at f_{EP})	3 mK	3 mK
Thermal gradients		
PSD (about f_{EP})	No	1 K m^{-1} $Hz^{-1/2}$
Tone (sine at f_{EP})	No	0.003 K m^{-1}

Table 2. Specifications to be met by the attitude control of the satellite and the compensation of its drag.

	Max. value at DC	Stability at f_{EP}
Ω angular velocity	10^{-5} rad s^{-1} or 2×10^{-3} rad s^{-1} (rotation)	10^{-5} rad s^{-1} Hz$^{-1/2}$
$d\Omega/dt$ angular acc.	3×10^{-7} rad s^{-2} (10^{-5} rad s^{-2} about Y)	3×10^{-8} rad s^{-2} Hz$^{-1/2}$
Γ linear acc.	3×10^{-9} m s^{-2}	3×10^{-10} m s^{-2} Hz$^{1/2}$

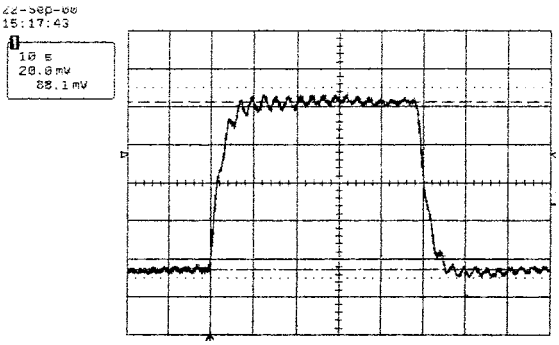

Figure 6. An indium thruster is tested in a vacuum chamber on a dedicated balance: a measurement of one 20 μN step of thrust is performed for several seconds; the residual oscillations are due to the balance's lack of damping.

frequency and the rotating frequency. The satellite's axis of rotation, and the normal to the orbital plane and to the accelerometer sensitive axes, have to be aligned with an accuracy of better than 10^{-3} rad, requiring alignments with respect to the star tracker mounted on the $Y+$ satellite face (see figure 5).

The satellite's residual acceleration and its attitude variations are specified because of the limited matching of the instrument sensitivities and alignments, and because of the mass residual off-centring. The drag-free and attitude control system (DFACS) will meet these requirements (table 2) by taking advantage of the accelerometer data (linear, but also angular, accelerations).

Four pods of two or three electric thrusters are to be installed on the corners of two opposite faces of the satellite. This configuration increases the delivered maximum torque that has to counteract the effect of the Earth's magnetic field on the residual magnetic moment of the satellite. Eight thrusters is the minimum number for full control, with 12 thrusters allowing total redundancy in the case of the failure of any one.

Each thruster must possess a maximum thrust range of 50–100 μN with a quantification step of 0.1 μN. Figure 6 presents thrust measurement performed in our laboratory with an indium thruster from ARCS (Seibersdorf, Austria) [17].

Because the DFACS needs the instrument data to operate, it is mandatory to ensure that the instrument is operating in safe mode when the drag compensation and the fine attitude control are not operating. Full ranges of operation, provided in table 3, are compatible with the satellite's on-orbit environment.

Table 3. Instrument range of operation in the two operating modes; performances for the EP test are obtained in measurement mode; resolution is a factor of 100 less in safe mode.

Accelerometer axes	Safe mode	Measurement mode
X (axial)	5×10^{-6} m s^{-2}	10^{-7} m s^{-2}
Y and Z (radial)	5×10^{-5} m s^{-2}	5×10^{-6} m s^{-2}
Rotation about X	10^{-5} rad s^{-2}	10^{-6} rad s^{-2}
Rotation about Y or Z	10^{-4} rad s^{-2}	10^{-5} rad s^{-2}

5. Experimental performance

The performance of the proposed experiment has being carefully analysed and simulations have been developed at the Côte d'Azur Observatory in order to assess the present error budget. Three types of errors have been considered: those from the instrument's operation, those from the instrument's environment and those from the satellite's motion and behaviour. For each source, stochastic and tone errors at the EP frequency or in its neighbourhood have been considered. Data process filtering efficiency has then to be taken into account. Orbit characteristics, satellite motion control, mass centring, sensitivity matching, thermal and magnetic environment have already been discussed above.

The instrument's performance is being evaluated in the light of previous analyses dedicated to the performance of the ultra-sensitive space accelerometers already developed for global and fine-structure recovery of the Earth's gravity field. These tri-axial electrostatic accelerometers, which have been designed and tested for the CHAMP [13] and GRACE [14] missions, are now being developed for the GOCE mission [18].

The resolution of the instrument is evaluated from the noise of the electronics circuits, as measured in the laboratory, from mass-motion sources of disturbance, as modelled after experimental investigations and from the environmental sensitivity. Resolution will be optimized at frequencies of around 10^{-3} Hz, i.e. several times the orbital frequency—corresponding to f_{EP}.

At frequencies lower than 10^{-3} Hz the thermal instabilities ΔT at the instrumental interface induce radiation pressure and radiometer acceleration fluctuations due, for the latter, to the residual gas pressure P inside the tight housing, i.e. in PSD:

$$\Gamma^2_{radiometer} \approx \left(\frac{1}{2m} P S \frac{\Delta T / \sqrt{1 + (2\pi \tau_e f_{EP})^2}}{T} \right)^2 \ (\mathrm{m\ s^{-2}})^2\ \mathrm{Hz^{-1}}$$

where m is the mass of the test mass, S is the area considered in the direction of the thermal gradient and τ_e is the thermal time constant from the interface to the core facing the test mass. With a pressure P of 10^{-5} Pa, a ΔT of 0.1 K Hz$^{1/2}$ and τ_e of 2 h, the radiometer effect is limited to 5×10^{-14} m s^{-2} Hz$^{1/2}$.

At frequencies higher than 10^{-2} Hz, the position sensing resolution x_{noise} affects the resolution with a square frequency law, i.e. in PSD:

$$\Gamma^2_{posnoise} = x^2_{noise} \left(4\pi^2 f^2_{EP} + 4\pi^2 f^2_p\right)^2 \ (\mathrm{m\ s^{-2}})^2\ \mathrm{Hz^{-1}}$$

where f_p is the frequency associated with the residual passive stiffness between the mass and the instrument structure (i.e. different from the active servo-loop one) which is evaluated to be less than 5×10^{-3} N m^{-1}—and so is negligible when effects have to be considered at lower frequencies.

About the frequency f_{EP} the thermal noise of the mass motion is the major source of error, being greater than the back-action of the electronics, the pick-up measurement noise,

or the magnetic or electric effects due to mass susceptibility or contact potential differences. Derived from the dissipation–fluctuation theorem, the expression depends on the damping factor (which does not include the electrostatic cold damping) estimated from dedicated laboratory experiments [19, 20], and found mainly to be due to the thin 5 μm wire used for the charge control of the mass, i.e. in PSD

$$\Gamma^2_{wire} = \left(\frac{1}{m} \sqrt{4k_b T \frac{k_{wire}}{2\pi f_{EP} Q_{wire}}} \right)^2 \quad (\mathrm{m\ s^{-2}})^2\ \mathrm{Hz^{-1}}$$

where k_{wire} and Q_{wire} are evaluated, respectively, to 10^{-5} N m^{-1} and 100 at 10^{-3} Hz, leading to 1.3×10^{-12} m s^{-2} Hz$^{-1/2}$. The quadratic sum of all considered noise sources then leads for each mass to 1.5×10^{-12} m s^{-2} Hz$^{-1/2}$, or less.

6. Conclusion

The definition of the MICROSCOPE space experiment has demonstrated the possibility of performing the EP test with a 10^{-15} accuracy, which is more than two orders of magnitude better than the present ground-based experiments. The as-performed measurement of the difference of accelerations will present a DSP of 2.1×10^{-12} m s^{-2} Hz$^{-1/2}$, which is sufficient to obtain the stated EP accuracy by integration of the signal over 20 h. The 120 kg satellite is specifically designed for the mission and the selected orbit is favourable for the stability of the instrument's thermal environment, and for the rejection of the Earth's gravity gradient signal.

Because of the satellite's drag compensation system, and its fine attitude control, the instrument will operate at a null, and its sensitivity is thereby much increased.

A prototype of the instrument is being produced to verify the technology involved which will take advantage of previous space accelerometer developments. The instrument needs a space environment to exhibit the required accuracy. Nevertheless, the prototype will operate in the laboratory under normal gravity, and it will enable the characterization of some driving parameters of the mechanical configuration, and of the electronics. Free-fall testing is also envisaged, specifically, in the drop tower of the University of Bremen [21]: 4 s of nanogravity observation are expected, but require a double capsule fall. The instrument's digital electronics will manage not only the mass' electrostatic control, but also all the procedures for calibration of the instrument in flight. These procedures are mandatory for the demonstration of the experiment's accuracy, and need to be verified through simulation software: the frequency aspects and the data filtering performance are now being studied with regard to the environment's spectral variations. The possibility of integration of the signals delivered by the instrument over weeks would lead to an accuracy of better than 10^{-15}.

Acknowledgments

The authors would like to acknowledge the MICROSCOPE team members at Onera, Observatoire de la Côte d'Azur, Cnes, and the University of Bremen, and in particular Gilles Métris and Bernard Tatry. The work described here was carried out with financial support from Cnes and Onera.

References

[1] Eddington A S 1922 *Mathematical Theory of Relativity* (Cambridge: Cambridge University Press)
[2] Nordtvedt K 1993 *Astrophys. J.* **407** 758

[3] Isham C J 1996 *Class. Quantum Grav.* **13** A5
[4] Haugan M P and Lammerzahl C 2000 Principles of equivalence: their role in gravitation physics and experiments that test them *Gyros, Clocks, Interferometers. . . : Testing Relativistic Gravity in Space (Lecture Notes in Physics)* (Berlin: Springer)
[5] Damour T and Polyakov A M 1994 *Nucl. Phys.* B **423** 532
[6] Baesler S *et al* 1999 Improved test of the equivalence principle for gravitational self energy *Phys. Rev. Lett.* **83** 18
[7] Dickey J O *et al* 1994 *Science* **265** 482
[8] Worden P W and Bye M 1996 *Class. Quantum Grav.* **13** A155
[9] Touboul P, Rodrigues M, Willemenot E and Bernard A 1996 Electrostatic accelerometers for the equivalence principle test in space *Class. Quantum Grav.* **13** A67
[10] Lockerbie N *et al* 2000 STEP: a status report *Gyros, Clocks, Interferometers. . . : Testing Relativistic Gravity in Space (Lecture Notes in Physics)* (Berlin: Springer)
[11] Everitt C W F *et al* 2000 *SMEX Mission Selected for Study: STEP Satellite Test of Equivalence Principle* NASA
[12] Touboul P *et al* 2000 Accelerometers for CHAMP, GRACE and GOCE *Boll. Geofis. Teor. Appl.* bg090
[13] Reigber C *et al* 2000 CHAMP mission status and perspectives *AGU Fall Meeting (San Francisco, CA)*
[14] 1998 GRACE: Science and Mission Requirements Document, revision A, JPL D-15928, NASA's Earth System Science Pathfinder Program
[15] Marcuccio S *et al* 1997 FEEP microthruster technology status and potential applications *AIAA*
[16] Fehringer M *et al* 1999 Micronewton indium thrusters *26th Int. Electric Propulsion Conf. (Kitakyushu)*
[17] Bonnet J *et al* 2000 Development of a thrust balance in the micro-newton range *3rd Int. Conf. Spacecraft Propulsion (Cannes)*
[18] 1999 Gravity field and steady state ocean circulation mission *ESA Publication* SP-1233-1
[19] Willemenot E 1997 Pendule de torsion. . . suspension électrostatique *Thesis* Université Orsay-Paris XI
[20] Josselin V 1999 Architecture mixte pour les accéléromètres ultrasensibles dédiés aux missions spatiales de physique fondamentale *Thesis* Université Orsay-Paris XI
[21] Dittus H 1991 Drop tower 'Bremen' a weightlessness laboratory on Earth *Endaveour New Series* **15** no 2